

# Electrochemical Synthesis, Properties, and Structure of 1,10-Phenanthroline Adducts of Mononuclear Copper, Cobalt, and Nickel Chelates in the N,N,O-Ligand Environment

D. A. Garnovskii<sup>a, \*</sup>, V. G. Vlasenko<sup>b</sup>, G. G. Aleksandrov<sup>c, †</sup>, S. I. Levchenkov<sup>a</sup>, N. I. Makarova<sup>d</sup>,  
Yu. V. Koshchienko<sup>d</sup>, A. I. Uraev<sup>d</sup>, and A. S. Burlov<sup>d</sup>

<sup>a</sup>Southern Scientific Center, Russian Academy of Sciences,  
Rostov-on-Don, 344006 Russia

<sup>b</sup>Research Institute of Physics, Southern Federal University,  
Rostov-on-Don, 344090 Russia

<sup>c</sup>Kurnakov Institute of General and Inorganic Chemistry, Russian Academy of Sciences,  
Moscow, 119991 Russia

<sup>d</sup>Research Institute of Physical and Organic Chemistry, Southern Federal University,  
Rostov-on-Don, 344090 Russia

\*e-mail: garn@ipoc.sfedu.ru

Received December 26, 2017

**Abstract**—1,10-Phenanthroline (Phen) adducts [M(L)Phen] in copper(II), cobalt(II), and zinc(II) chelates based on N,N,O-tridentate tosylamino-functionalized pyrazole-containing Schiff base (H<sub>2</sub>L), resulting from condensation of 2-tosylaminoaniline with 3-methyl-1-phenyl-4-formylpyrazol-5-ol, were obtained by electrosynthesis. The composition and structure of the mixed-ligand complexes were confirmed by elemental analysis, IR spectroscopy, and magnetochemical measurements. The structures of azomethine H<sub>2</sub>L and mixed-ligand copper(II) complex were determined by X-ray diffraction.

**Keywords:** electrosynthesis, mixed-ligand complexes, 1,10-phenanthroline, tridentate Schiff bases, X-ray diffraction

**DOI:** 10.1134/S1070328418100032

## INTRODUCTION

1,10-Phenanthroline (Phen) and its derivatives are common bidentate N,N-heterocyclic bases that chelate metal ions, which accounts for the persistent interest in these compounds as diverse precursors for organic, coordination, inorganic, and supramolecular chemistry [1–3]. Owing to the structural and chemical (hydrophobicity, planarity, electron deficiency) features of phenanthroline, its metal complexes exhibit catalytic, redox, and photochemical properties [4, 5]. Furthermore, the use of phenanthroline and its derivatives as ligands may serve for targeted design of luminescent compounds and photoswitchable molecular systems [6]. Complexes based on functionalized Phen compounds have been found to exhibit sensing properties. They can be used as model compounds to study protein binding/cleavage in natural objects [3].

The present study is devoted to electrosynthesis, physicochemical properties, and structure of 1,10-phenanthroline adducts of copper(II) (**I**), cobalt(II) (**II**), and nickel(II) (**III**) chelates based on tridentate N,N,O-sulfonamide pyrazole-containing Schiff base.

## EXPERIMENTAL

Commercially available (Alfa Aesar) solvents and metal plates (2 × 2 cm) were used. *N*-(2-{[3-methyl-5-oxo-1-phenyl-1,5-dihydro-4*H*-pyrazol-4-ylidene)methyl]amino}phenyl-4-methylbenzenesulfonamide (H<sub>2</sub>L) and 2-tosylaminoaniline were synthesized by previously described procedures [7, 8].

**Electrosynthesis** was performed by a standard common procedure [9] using a EG&GPAR/173 potentiostat in a methanol–acetonitrile (1 : 1) mixture with a

† Deceased.

platinum cathode and a metal (Cu, Co, Ni) plate as an anode. The working solution (25 mL) contained  $H_2L$  (0.223 g, 0.5 mmol), Phen (0.090 g, 0.5 mmol), and  $Et_4NClO_4$  (0.020 g) as the electrolyte. The electrolysis was carried out in a undivided U-shaped glass cell at 19 mA and initial voltage of 10 V for 1.3 h. After the electrolysis, the precipitates of the complexes were filtered off, washed with hot isopropanol, and dried in *vacuo*.

**Complex I:** green crystals. Yield 0.254 g (74%).  $T_m = 182\text{--}184^\circ\text{C}$ .

For  $C_{36}H_{28}N_6O_3SCu$

Anal. cacl., %	C, 62.79	H, 4.07	N, 12.21
Found, %	C, 62.19	H, 4.12	N, 12.14

IR (KBr;  $\nu$ ,  $\text{cm}^{-1}$ ): 1620 s  $\nu(\text{C}=\text{N})$ , 1608 s  $\nu(\text{C}=\text{N})$ , 1331 s  $\nu_{as}(\text{SO}_2)$ , 1137 s  $\nu_s(\text{SO}_2)$ .

The single crystals of complex I suitable for X-ray diffraction were obtained by slow evaporation of the methanol–acetonitrile solution (1 : 1).

**Complex II:** brown crystals. Yield 0.189 g (55%).  $T_m = 191\text{--}193^\circ\text{C}$  (dec.).

For  $C_{36}H_{28}N_6O_3SCo$

Anal. cacl., %	C, 63.85	H, 4.10	N, 12.29
Found, %	C, 63.26	H, 4.37	N, 12.36

IR (KBr;  $\nu$ ,  $\text{cm}^{-1}$ ): 1617 s  $\nu(\text{C}=\text{N})$ , 1605 s  $\nu(\text{C}=\text{N})$ , 1351 s  $\nu_{as}(\text{SO}_2)$ , 1146 s  $\nu_s(\text{SO}_2)$ .

**Complex III:** brown crystals. Yield 0.236 g (69%).  $T_m = 174\text{--}177^\circ\text{C}$  (dec.).

For  $C_{36}H_{28}N_6O_3SNi$

Anal. cacl., %	C, 63.91	H, 4.12	N, 12.31
Found, %	C, 63.60	H, 4.36	N, 12.42

IR (KBr;  $\nu$ ,  $\text{cm}^{-1}$ ): 1619 s  $\nu(\text{C}=\text{N})$ , 1607 s  $\nu(\text{C}=\text{N})$ , 1344 s  $\nu_{as}(\text{SO}_2)$ , 1162 s  $\nu_s(\text{SO}_2)$ .

Elemental analysis (C,H,N) was performed on a TCM 480 Carlo Erba instrument. The IR spectra for samples as KBr pellets were measured on a Nicolet Impact-400 instrument in the 4000–400  $\text{cm}^{-1}$  range. Melting points were measured on a Kofler stage. The specific magnetic susceptibility was determined by the relative Faraday method at room temperature;  $Hg[\text{Co}(\text{CNS})_4]$  was used as the reference for calibration.

**The X-ray diffraction study** of  $H_2L$  and I was carried out on a Bruker SMART APEX2 CCD diffractometer ( $MoK_\alpha$ ,  $\lambda = 0.71073 \text{ \AA}$ , graphite monochromator,  $\omega$ -scan mode). The initial array of measured

intensities was processed using the SAINT and SADABS programs included in the APEX2 package [10, 11]. The structure of  $H_2L$  was determined by a combination of direct methods and Fourier syntheses. The hydrogen atoms at the N atoms were located objectively from difference Fourier syntheses; the positions of H atoms at C atoms were calculated geometrically. The structure of complex I was solved by direct methods and refined by full-matrix least-squares calculations in the anisotropic approximation for non-hydrogen atoms on  $F_{hkl}^2$ . The hydrogen atoms were placed into geometrically calculated positions.

The structure solution and refinement were performed using the SHELXTL program package [12]. The X-ray experiment details and crystallographic data for  $H_2L$  and I are summarized in Table 1 and selected interatomic distances and bond angles are presented in Table 2. The structures of compounds were analyzed using the PLATON program [13].

The atom coordinates and thermal factors for  $H_2L$  and I are deposited with the Cambridge Crystallographic Data Centre (CCDC nos. 1811271 and 1811269, respectively; [deposit@ccdc.cam.ac.uk](mailto:deposit@ccdc.cam.ac.uk) or [http://www.ccdc.cam.ac.uk/data\\_request/cif](http://www.ccdc.cam.ac.uk/data_request/cif)).

## RESULTS AND DISCUSSION

Taking into account our previous results [14–16] dealing with the coordination ability of tridentate tosylamino-functionalized pyrazole-containing Schiff bases with different sets of N,N,O- or N,N,S-donor centers in the presence of adduct-forming aminoheterocyclic compounds during electrooxidation of various 3d metals, we accomplished electrosynthesis of a series of adducts of copper(I), cobalt(II), and nickel(III) chelates with 1,10-phenanthroline acting as the co-ligand.

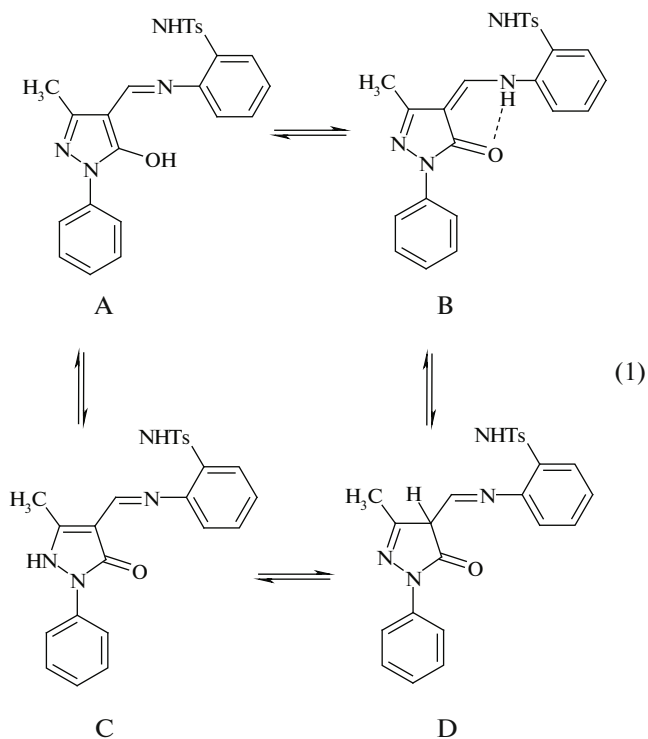
Azomethine derivatives of 4-formyl-3-methyl-1-phenylpyrazol-5-ol are known to exist as several tautomers [17–21]. To compare their relative stability, we calculated the total energy of tautomers A–D (Scheme 1) in the gas phase by quantum chemical methods using the Gaussian-03 program [22], the Becke–Lee–Yang–Parr (B3LYP) hybrid functional [23, 24] and the standard 6-31G(d,p) basis set (Table 3).

**Table 1.** Crystal data and X-ray experiment and structure refinement details for H<sub>2</sub>L and complex **I**

Parameter	Value	
	H <sub>2</sub> L	<b>I</b>
Molecular formula	C <sub>24</sub> H <sub>22</sub> N <sub>4</sub> O <sub>3</sub> S	C <sub>37</sub> H <sub>29.50</sub> N <sub>6.50</sub> O <sub>3</sub> SCu
<i>M</i>	446.51	708.77
Crystal size, mm	0.40 × 0.34 × 0.15	0.24 × 0.16 × 0.14
Temperature, K	120	123
System	Monoclinic	Monoclinic
Space group	<i>P</i> 2 <sub>1</sub> /c	<i>P</i> 2 <sub>1</sub> /n
<i>a</i> , Å	14.2324(7)	14.4880(6)
<i>b</i> , Å	8.9157(4)	13.6926(6)
<i>c</i> , Å	17.11329(9)	15.9925(7)
β, deg	92.1412(10)	90.2407(7)
<i>V</i> , Å <sup>3</sup>	2172.51(18)	3172.5(2)
<i>Z</i>	4	4
ρ(calcd.), g/cm <sup>3</sup>	1.365	1.484
μ, mm <sup>-1</sup>	0.184	0.807
<i>F</i> (000)	936	1464
Scanning range in θ, deg	3.0–28.2	2.4–29.1
Number of measured reflections	25610	25490
Number of unique reflections	5774	8448
Number of reflections with <i>I</i> > 2σ( <i>I</i> )	4786	7347
Ranges of reflection indices	–19 < <i>h</i> < 19, –12 < <i>k</i> < 12, –23 < <i>l</i> < 23	–19 < <i>h</i> < 19, –17 < <i>k</i> < 18, –21 < <i>l</i> < 21
Number of refined parameters	300	437
<i>R</i> <sub>1</sub> ( <i>I</i> > 2σ( <i>I</i> ))	0.0374	0.033
<i>wR</i> <sub>2</sub> (all reflections)	0.1021	0.111
GOOF (all reflections)	1.005	1.000
Δρ <sub>max</sub> /Δρ <sub>min</sub> , e Å <sup>–3</sup>	0.368/–0.497	0.48/–0.43

**Table 2.** Selected interatomic distances (*d*) and bond angles ( $\omega$ ) in the molecules of  $\text{H}_2\text{L}$  and **I**

Bond	<i>d</i> , Å	Bond	<i>d</i> , Å
<b><math>\text{H}_2\text{L}</math></b>			
S(1)–O(2)	1.4340(11)	N(2)–N(2)	1.4095(15)
S(1)–O(3)	1.4330(11)	N(2)–C(1)	1.3895(16)
S(1)–N(4)	1.6429(11)	N(2)–C(4)	1.4124(17)
S(1)–C(17)	1.6429(11)	N(3)–C(10)	1.3274(16)
O(1)–C(1)	1.2475(15)	N(3)–C(11)	1.4063(16)
N(1)–C(3)	1.3057(18)	N(4)–C(12)	1.4361(16)
<b>I</b>			
Cu(1)–N(2)	1.9537(11)	Cu(1)–N(1)	2.0259(12)
Cu(1)–O(1)	1.9779(11)	Cu(1)–N(6)	2.2887(12)
Cu(1)–N(5)	2.0079(11)		
Angle	$\alpha$ , deg	Angle	$\alpha$ , deg
<b><math>\text{H}_2\text{L}</math></b>			
C(3)N(1)N(2)	106.40(10)	O(2)S(1)O(3)	120.69(7)
C(1)N(2)N(1)	111.91(11)	O(2)S(1)N(4)	104.72(6)
C(1)N(2)C(4)	129.98(11)	O(3)S(1)N(4)	106.86(6)
N(1)N(2)C(4)	118.08(10)	O(2)S(1)C(17)	107.81(6)
C(10)N(3)C(11)	127.12(12)	O(3)S(1)C(17)	109.04(6)
O(1)C(1)N(2)	127.18(12)	N(4)S(1)C(17)	106.92(6)
O(1)C(1)C(2)	128.84(12)	C(12)N(4)S(1)	120.69(9)
<b>I</b>			
N(2)Cu(1)O(1)	94.33(4)	N(5)Cu(1)N(1)	101.95(4)
N(2)Cu(1)N(5)	177.10(4)	N(2)Cu(1)N(6)	101.58(5)
O(1)Cu(1)N(5)	82.94(4)	O(1)Cu(1)N(6)	104.20(5)
N(2)Cu(1)N(1)	80.94(4)	N(5)Cu(1)N(6)	78.20(5)
O(1)Cu(1)N(1)	163.62(5)	N(1)Cu(1)N(6)	92.14(5)



Scheme 1.

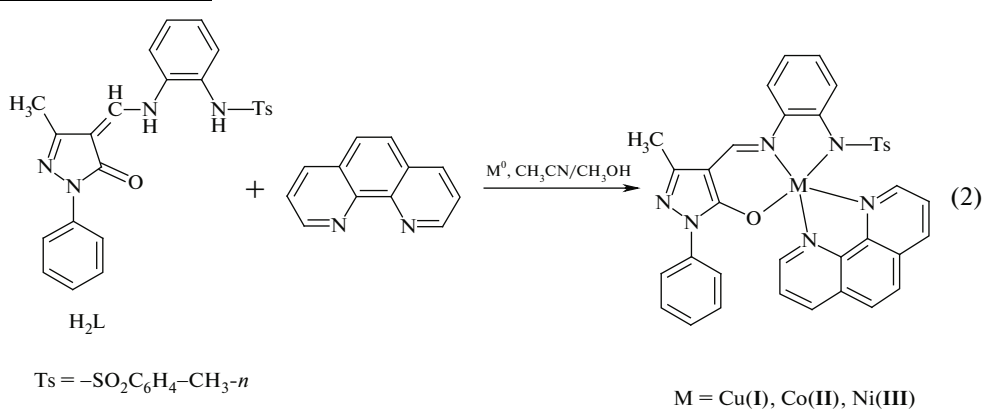
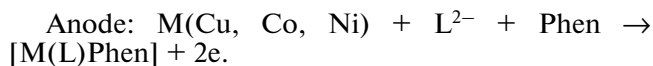
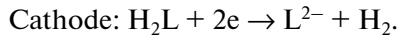
The keto-enamine form B was found to be most stable, as was shown previously in experiments (IR and  $^1\text{H}$  NMR spectra) [15].

The anodic dissolution of copper, cobalt, and nickel during electrolysis in a methanol–acetonitrile (1 : 1) solution containing an N,N,O-tridentate Schiff base  $\text{H}_2\text{L}$  and an equimolar amount of Phen results in the formation of mononuclear mixed-ligand complexes  $[\text{M}(\text{L})\text{Phen}]$  ( $\text{M} = \text{Cu(I)}, \text{Co(II)}, \text{and Ni(III)}$ ) in which  $\text{L}^{2-}$  is the dianion of the  $\text{H}_2\text{L}$  ligand (Scheme 2).

The overall process occurring in the electrolytic cell can be represented as follows:



Electrosynthesis of the complexes:



Scheme 2.

The IR spectra of complexes **I–III**, in comparison with the IR spectrum of the free azomethine  $\text{H}_2\text{L}$ , do not contain  $\nu(\text{N–H})$  stretching bands of the tosylated

amino group at  $3215 \text{ cm}^{-1}$  and  $\nu(\text{C=O})$  stretching bands for the vinylogous oxoamide group in the  $\text{C}(\text{=O})-\text{CH}=\text{CHN}$  moiety at  $1655 \text{ cm}^{-1}$  [15];

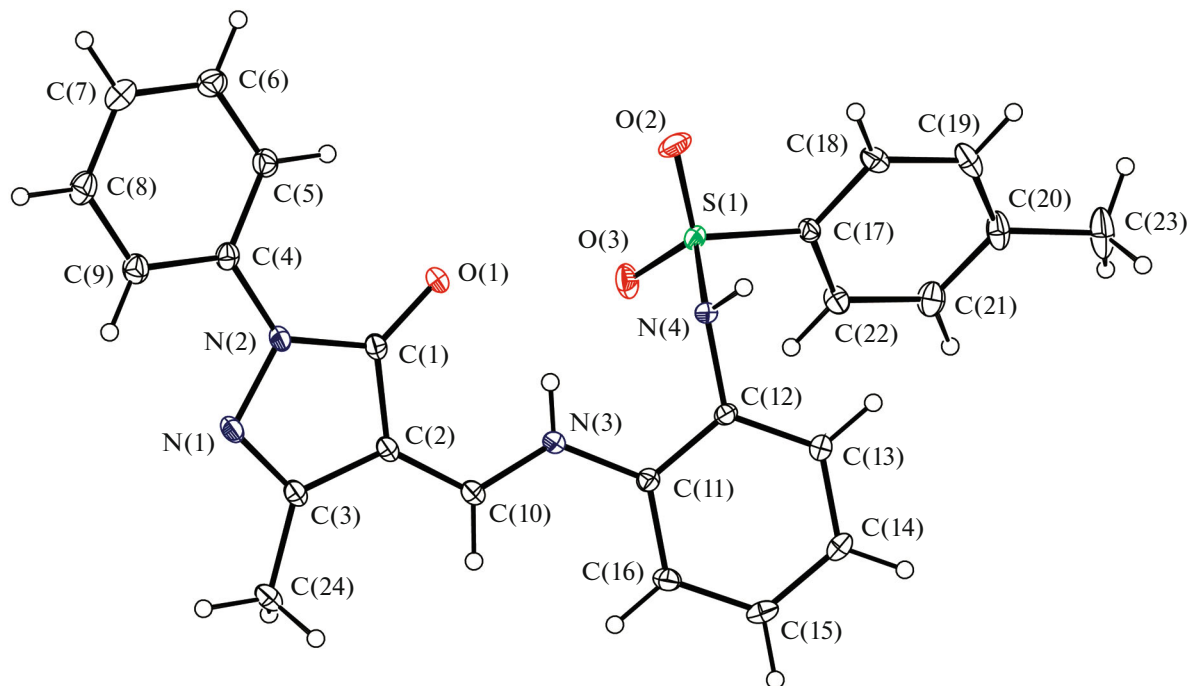


**Fig. 1.** Molecular structure of  $\text{H}_2\text{L}$  with atoms being represented by thermal ellipsoids at 50% probability.

instead,  $\nu(\text{C}=\text{N})$  stretching bands appear at 1620 (**I**), 1617 (**II**), and 1619 (**III**). The IR spectral data suggest that  $\text{H}_2\text{L}$  is involved in complex formation as doubly deprotonated ( $\text{L}^{2-}$ ) enol imine form. The coordination bonds are localized on the tosylated amino group

nitrogen, imine nitrogen, and deprotonated hydroxy group oxygen, thus forming the  $\{\text{M}\text{N}_2\text{O}\}$  coordination unit.

The mononuclear structure of the adducts was confirmed by magnetochemical measurements performed at 293 K ( $\mu_{\text{eff}} = 1.95, 4.19$ , and  $3.26 \mu_{\text{B}}$  for **I**–**III**, respectively). The final conclusion about the structure of the heteroaromatic Schiff base  $\text{H}_2\text{L}$  and complex **I** was derived from X-ray diffraction data.

The molecular structure of  $\text{H}_2\text{L}$  is shown in Fig. 1. The phenyl substituent at the N(2) atom is somewhat rotated relative to the pyrazole ring plane; the C(9)–C(4)–N(2)–N(1) torsion angle is  $8.25^\circ$ . The N(3)–C(10) bond lies virtually in the pyrazole ring plane. The dihedral angle between the mean planes of the pyrazole and C(11)C(12)C(13)C(14)C(15)C(16) rings is  $15.9^\circ$ .

**Table 3.** Relative energies of tautomers of  $\text{H}_2\text{L}$

Tautomer	Relative energy, kcal/mol (gas phase)
A	6.99
B	0
C	21.83
D	21.59

**Table 4.** Geometric parameters of hydrogen bonds in the single crystal of  $\text{H}_2\text{L}^*$

D–H···A	Distance, Å			DHA angle, deg
	D–H	H···A	D···A	
N(3)–H(3N)···O(1)	0.836(18)	2.206(18)	2.8630(15)	135.6(15)
N(3)–H(3N)···N(4)	0.836(18)	2.348(17)	2.7466(16)	109.9(14)
N(4)–H(4N)···O(1) <sup>i</sup>	0.837(19)	2.255(19)	3.0599(16)	161.5(17)

\* Symmetry codes: <sup>i</sup>  $1 - x, 1 - y, 1 - z$ .

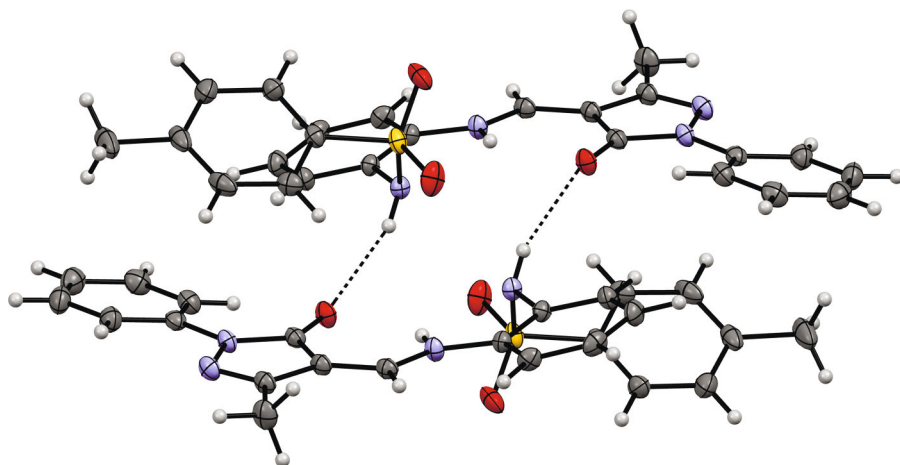


Fig. 2. Centrosymmetric hydrogen-bonded dimers of  $\text{H}_2\text{L}$ .

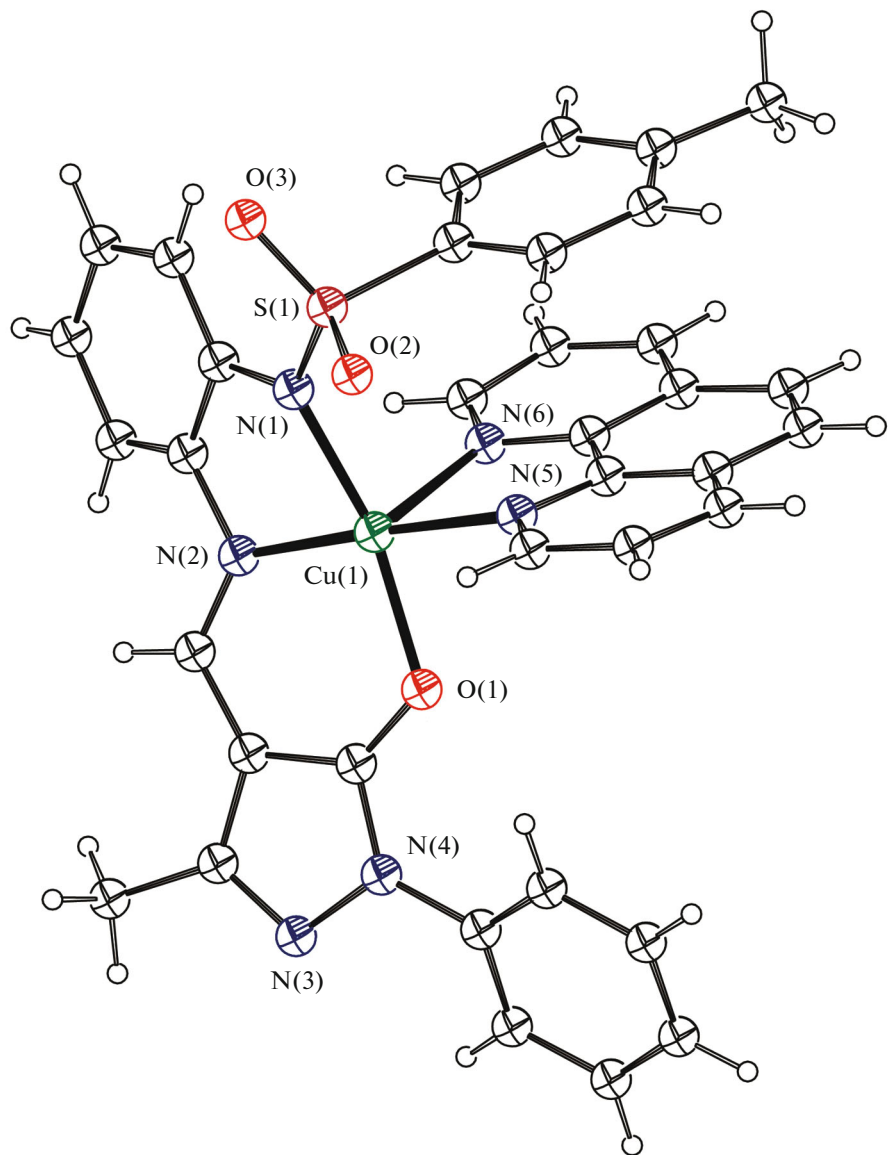


Fig. 3. Molecular structure of complex I with atoms being represented by thermal ellipsoids at 30% probability; acetonitrile molecule is not shown.

In the  $\text{H}_2\text{L}$  molecule, there are two intramolecular hydrogen bonds (HBs): the relatively strong  $\text{N}(3)-\text{H}(3\text{N})\cdots\text{O}(1)$  bond and weaker  $\text{N}(3)-\text{H}(3\text{N})\cdots\text{N}(4)$  bond (Table 4). Also, the intermolecular  $\text{N}(4)-\text{H}(4\text{N})\cdots\text{O}(1)^i$  hydrogen bond is present in the single crystal, thus giving rise to hydrogen-bonded centrosymmetric dimers (Fig. 2).

The structure of complex **I** molecule  $[\text{Cu}(\text{L})\text{Phen}]$  is depicted in Fig. 3. The coordination polyhedron of the copper ion can be defined as an extended square pyramid. The equatorial positions are occupied by the  $\text{N}(1)$  and  $\text{N}(2)$  amine atoms, the  $\text{O}(1)$  atom of the oxopyrazole moiety, and the  $\text{N}(5)$  atom of the coordinated Phen molecule. The  $\text{O}(1)$  atom is markedly (by 0.544 Å) deviated from the plane through the other donor atoms. The apical position is occupied by the phenanthroline  $\text{N}(6)$  atom. The structure of the complex includes also 0.5 acetonitrile molecules, which occupy voids in the crystal cell.

The five-membered metallacycles  $\text{Cu}(1)\text{N}(1)\text{C}(1)\text{C}(6)\text{N}(2)$  and  $\text{Cu}(1)\text{N}(5)\text{C}(36)\text{C}(35)\text{N}(6)$  have an envelope conformation, with the flap being formed by the  $\text{Cu}(1)$  atom deviating from the mean planes of the other ring atoms by 0.674 and 0.199 Å, respectively. The six-membered chelate ring is in the half-boat conformation, with the  $\text{Cu}(1)$  atom deviating from the mean plane through the other atoms by 0.216 Å.

The benzene ring of the tosylamine moiety and the Phen molecule are involved in  $\pi$ -stacking interaction; the dihedral angle between the mean planes is 5.74° and the shortest inter-centroid distance is 3.521 Å.  $\pi$ -Stacking interaction occurs also between the Phen ligands of the neighboring complex molecules; the dihedral angle between the mean planes of the interacting rings is 3.54° and the shortest inter-centroid distance is 3.669 Å.

1,10-Phenanthroline adducts of copper, cobalt, and nickel chelates based on the  $\text{N},\text{N},\text{O}$ -tridentate pyrazole-containing Schiff base were prepared by electrooxidation of copper, cobalt, and nickel. The structure and composition of the complexes were confirmed by combination of IR spectral, magnetochemical, and X-ray diffraction data (azomethine  $\text{H}_2\text{L}$  and copper complex **I**).

#### ACKNOWLEDGMENTS

Experimental data were obtained using equipment of the Center for Collective Use “Molecular Spectroscopy” of the Southern Federal University.

The authors are grateful to Dr.Sc. (chemistry), Professor of the RAS, K.A. Lysenko for highly skilled X-ray diffraction measurements and interpretation and discussion of X-ray diffraction results.

This work was supported by the Southern Scientific Center, Russian Academy of Sciences (government order no. 01201354239) and the Russian Foundation for Basic Research (grant no. 16-03-00503a).

#### REFERENCES

1. Sammers, P.G. and Yahioglu, G., *Chem. Soc. Rev.*, 1994, vol. 23, no. 2, p. 327.
2. Luman, C.R. and Castellano, F.N., in *Comprehensive Coordination Chemistry*, McCleverty, J.A., Meyer, T.J., and Lever, A.B.P., Eds., Oxford: Elsevier, 2004, vol. 1, p. 25.
3. Benchini, A. and Lippolis, V., *Coord. Chem. Rev.*, 2010, vol. 254, nos. 17–18, p. 2096.
4. Bossert, J. and Daniel, C., *Coord. Chem. Rev.*, 2008, vol. 252, nos. 23–24, p. 2493.
5. Zhang, Y., Shulz, M., Wächtler, M., et al., *Coord. Chem. Rev.*, 2018, vol. 356, p. 127.
6. Accorsi, G., Listorti, A., Yoosaf, K., and Armaroli, N., *Chem. Soc. Rev.*, 2009, vol. 38, p. 1690.
7. Garnovskii, D.A., Antsyshkina, A.S., Churakov, A.V., et al., *Russ. J. Inorg. Chem.*, 2014, vol. 59, p. 431. doi 10.1134/S0036023614050088
8. Malick, W.U. and Sharma, T.S., *J. Indian Chem. Soc.*, 1970, vol. 47, no. 2, p. 167.
9. Tuck, D.G., *Pure Appl. Chem.*, 1979, vol. 51, no. 10, p. 2005.
10. *SMART and SAINT. Release 5.0. Area Detector Control and Integration Software*, Madison: Bruker AXS, 1998.
11. Sheldrick, G.M., *SADABS. A Program for Exploiting the Redundancy of Area-Detector X-ray Data*, Göttingen: Univ. of Göttingen, 1999.
12. Sheldrick, G.M., *Acta Crystallogr., Sect. A: Found. Crystallogr.*, 2008, vol. 64, no. 1, p. 112.
13. Spek, A.L., *J. Appl. Crystallogr.*, 2003, vol. 36, no. 1, p. 7.
14. Garnovskii, D.A., Antsyshkina, A.S., Makarova, N.I., et al., *Russ. J. Inorg. Chem.*, 2015, vol. 60, p. 1528. doi 10.1134/S0036023615120116
15. Garnovskii, D.A., Aleksandrov, G.G., Makarova, N.I., et al., *Russ. J. Inorg. Chem.*, 2017, vol. 62, p. 1077. doi 10.1134/S0036023617080071
16. Vlasenko, V.G., Garnovskii, D.A., Aleksandrov, G.G., et al., *Polyhedron*, 2017, vol. 133, p. 245.
17. Antsyshkina, A.S., Sadikov, G.G., Uraev, A.I., et al., *Crystallogr. Rep.*, 2000, vol. 45, no. 5, p. 778.
18. Jadeja, R.N., Snan, J.R., Suresh, E., and Parimal, P., *Polyhedron*, 2004, vol. 23, no. 16, p. 2465.
19. Xu, G.-C., Zhang, L., Liu, L., et al., *Polyhedron*, 2008, vol. 27, no. 1, p. 12.
20. Casas, J.S., Garcia-Tasende, M.S., Sanchez, A., et al., *Coord. Chem. Rev.*, 2007, vol. 251, nos. 11–12, p. 1561.
21. Levchenkov, S.A., Shcherbakov, I.N., Popov, L.D., et al., *Inorg. Chim. Acta*, 2013, vol. 405, p. 169.
22. Frisch, M.J., Trucks, G.W., Schlegel, H.B., et al., *Gaussian 03. Revision A1*, Pittsburgh: Gaussian Inc., 2003.
23. Becke, A.D., *J. Chem. Phys.*, 1993, vol. 98, p. 5648.
24. Lee, C., Yang, W., and Parr, R.G., *Phys. Rev.*, 1988, vol. 37, p. 785.

Translated by Z. Svitanko